Progress In Electromagnetics Research C, Vol. 138, 233–246, 2023

Circularly Polarized Gap-Coupled Designs of Modified Square Microstrip Antennas for WLAN and Bluetooth Applications

Amit A. Deshmukh*, Venkata A. P. Chavali, and Aarti G. Ambekar

Abstract—Circularly polarized gap-coupled designs of corner truncated square microstrip antenna in 2400 MHz frequency spectrum are presented. The gap-coupled design on thinner substrate ($\sim 0.036\lambda_g$) yields axial ratio bandwidth of 113 MHz (4.697%) whereas that on thicker substrate ($\sim 0.13\lambda_g$) yields axial ratio bandwidth of 471 MHz (19.24%). Both the designs exhibit broadside radiation pattern with a peak gain above 7 dBi, thus satisfying the requirements of WLAN and Bluetooth applications. Simulated results have been experimentally verified, which show close agreement.

1. INTRODUCTION

With numerous advantages, microstrip antenna (MSA) finds many applications in various communication systems [1, 2]. In point-to-point applications, signals travel through the multiple paths that affects its polarization. To minimize the signal loss arising due to this polarization mismatch, circularly polarized (CP) antennas are preferred, in which MSA is largely preferred, as a single patch configuration with suitable alterations in the geometry can yield CP characteristics [1, 2]. The CP response in MSA is achieved by using different techniques like cutting a narrow slot, placing a stub, use of a power divider circuit with dual feeds, by employing modified shapes of the patch, regular patch geometries employing resonant slots, and modified shapes of the ground plane [3–16]. The axial ratio (AR) bandwidth (BW) and gain in CP designs are increased either by employing thicker substrates or by using multiple patches in the same or stacked layer or by using array designs [17–26]. Of all the methods reported, the use of multiple patches is the simplest technique to increase the AR BW.

This paper presents gap-coupled designs of a corner truncated square MSA (SMSA) for wideband CP response on thinner and thicker substrates. Initially, the CP design of SMSA is presented in 1300 MHz frequency band on an air suspended FR4 substrate ($\varepsilon_r = 4.3$, $h = 0.16$ cm) having electrical thickness $< 0.03\lambda_g$. The truncation of the patch corner degenerates TM_{10} mode of the square patch into dual diagonal resonant modes that yields AR BW of 1.37%, offering broadside gain of 7 dBi. An increase in the AR BW is further obtained by using the gap-coupled configurations, in which additional parasitic patches are coupled to the fed patch. With the patches gap-coupled along the y-axis, AR BW of 4.2% is achieved showing broadside gain characteristics. Based on these designs, methodology to implement similar gap-coupled CP MSAs is developed. A single patch antenna designed using the same in 2400 MHz band on substrate thickness of $< 0.03\lambda_g$ yields AR BW of 1.8%. In the same frequency band, gap-coupled design with patches coupled along y-axis yields an AR BW of 4.6% with a broadside gain of more than 7 dBi. To enhance the AR BW, a thicker substrate design is presented in 2400 MHz frequency band. The MSA fed using a proximity strip of thickness $\sim 0.13\lambda_g$ yields an AR BW of nearly 20% with a broadside gain greater than 7 dBi. Thus, using a simple gap-coupled multi-resonator technique, an AR BW of nearly 20% is achieved. To highlight the technical novelty, a comparison of the proposed antenna against the reported wideband CP MSAs is presented. It shows

Received 14 August 2023, Accepted 27 October 2023, Scheduled 10 November 2023
* Corresponding author: Amit A. Deshmukh (amitdeshmukh76@gmail.com).
The authors are with the EXTC, SVKM's D J Sanghvi CoE, Mumbai, India.

that in terms of the technique used, the proposed thicker substrate design offers optimum results for AR BW. With the achieved antenna characteristics, the proposed MSA can find applications in WLAN and Bluetooth applications in 2400 MHz frequency band. The configurations presented in this paper were initially optimized using IE3D simulations [27] that was followed by experimental verifications using the instruments like ZVH — 8, SMB 100A and FSC 6. The measurement was carried out inside an Antenna lab.

2. GAP-COUPLED CORNER TRUNCATED SMSAS FOR CP RESPONSE

The design of gap-coupled variation of corner truncated SMSAs is shown in Figs. 1(a) and (b). Initially, the single patch design is studied. The square patch is fabricated on a suspended FR4 substrate ($h = 0.16$ cm, $\varepsilon_r = 4.3$) with an air gap $h_a = 0.32$ cm, thus realizing the total substrate thickness of 0.48 cm.

For this thickness and the feed position shown, using IE3D simulations, square patch length L_p ($L_p = W_p$) is optimized for TM_{10} mode frequency of 1350 MHz. The patch length is found to be 8.4 cm. To degenerate the orthogonal modes, a parametric study for the increase in truncation length 'd' is carried out, and the resonance curve, AR BW plots, and surface current distributions at the degenerated modes are shown in Figs. 1(c)–(f). The truncation of patch corners creates two unequal path lengths along the patch diagonal axis. Surface currents at the two modes show half wavelength variation along two diagonal axes. Hence, they are referred to as TM_{10}^{135} and TM_{01}^{45}. An optimum separation between them yields CP response as shown in Fig. 1(g). Antenna dimensions in the optimum design are $W_p = L_p = 8.4$, $d = 0.9$, $x_f = 2.2$ cm. The simulated and measured impedance BWs for $S_{11} < -10$ dB are 100 MHz (7.117%) and 103 MHz (7.36%), respectively. The CP AR BWs observed in the simulation and measurement are 19 MHz (1.376%) and 22 MHz (1.6%), respectively. The antenna offers a broadside radiation pattern over the AR BW showing equal contributions of co- and cross-polarization radiation components. Broadside antenna gain is more than 6 dBi across the AR BW. To increase the AR BW, multi-resonator concept is used, and the parasitic truncated square patches are gap-coupled to the fed patch as shown in Fig. 1(a). An increase in the AR BW is realized when the spacing between the resonant modes on the fed and parasitic patches is optimized. This inter-spacing is decided by the dimensions of parasitic patches with reference to the fed patch and an angle 'θ_y' & 'θ_x' in between them.

For the design with patches gap-coupled along y-axis, a parametric study for the variation in patch lengths (L_y) along y-axis and an angle θ_y between them as shown in Fig. 1(a) is carried out. The plots for them are shown in Figs. 2(a)–(d). Here, $L_y = W_y$ & $L_p = W_p$. The decrease in the parasitic patch dimensions increases the inter-spacing in between the orthogonal mode frequencies across the fed and parasitic patches. An angular separation between the patches optimizes the impedance at the modes to yield maximum possible AR BW. For the same fed patch parameters, an optimum AR BW is achieved for the parasitic patch parameters as $W_y = L_y = 8.2$, $d_y = 0.6$ cm, $\theta_y = 40^\circ$. Results for the gap-coupled SMSAs along y-axis are shown in Fig. 3. The simulated and measured impedance BWs are 90 MHz (6.475%) and 92 MHz (7.209%), respectively. The CP AR BWs in the simulation and measurement are 58 MHz (4.193%) and 61 MHz (4.418%), respectively. Gap-coupled antenna offers broadside radiation characteristics with peak gain of more than 8 dBi. The impedance BW is lower in this design, as the configuration is optimized for the maximum AR BW. The gap-coupled configurations with patches along x-axis and x & y-axfes were studied. Resultant AR BW in the two designs is lower than that obtained in the design with patches gap-coupled along y-axis. Hence, their results are not discussed here.

3. DESIGN METHODOLOGY FOR GAP-COUPLED CORNER TRUNCATED SMSAS

In this section, the methodology to design similar corner truncated CP SMSA variations is presented. The equations/parametric relations presented here are based on the optimum designs of single and gap-coupled patches discussed above. Initially, the desired center frequency of the AR BW 'f_{AR}' is specified, using which and Equation (1), TM_{10} mode frequency of SMSA is calculated. In the design, a two layer

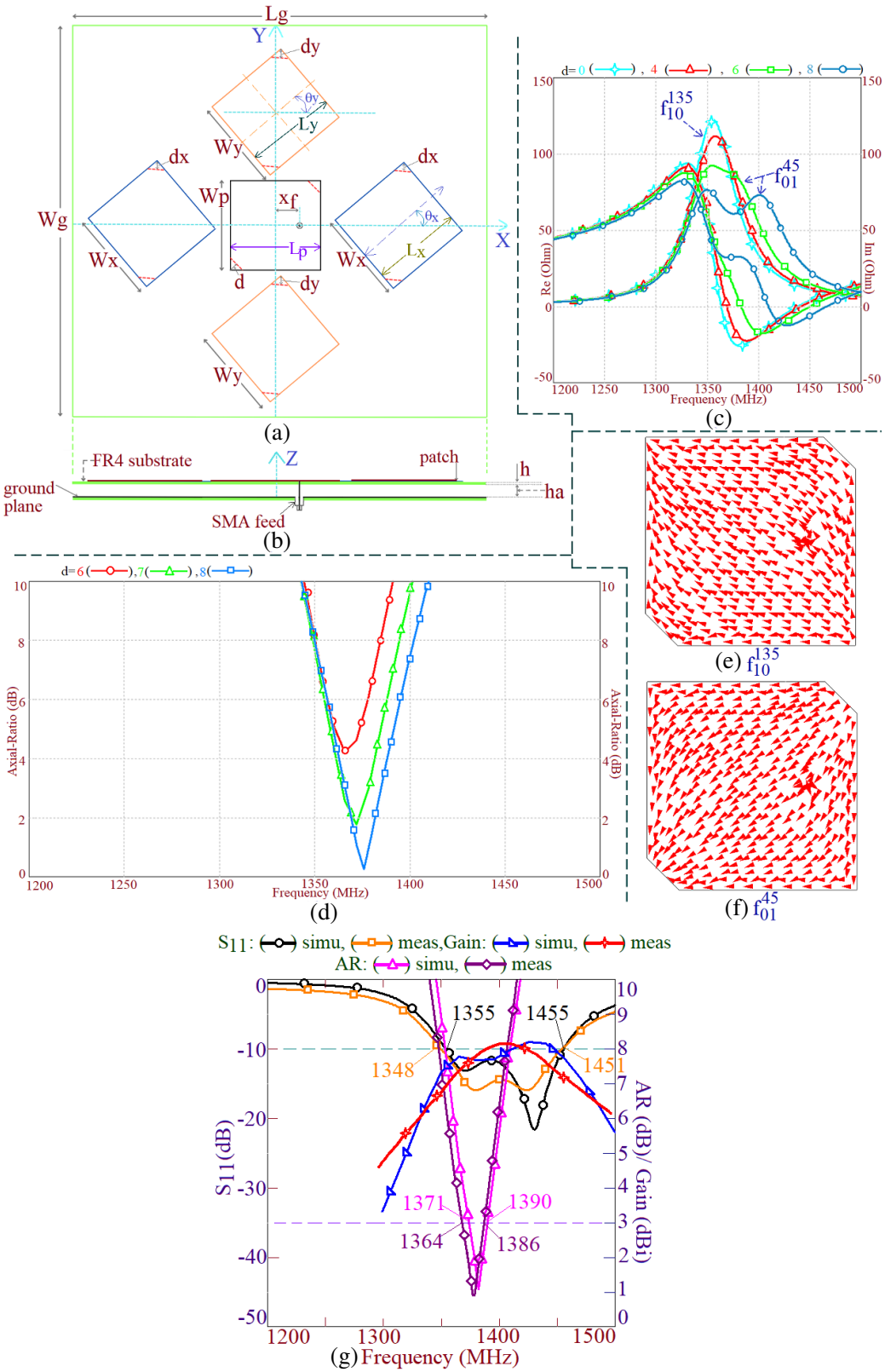

Figure 1. (a), (b) Gap-coupled design of corner truncated SMSAs, its (c) resonance curve, (d) AR BW plots, (e), (f) surface current distribution at degenerated modes and its (g) optimum results.

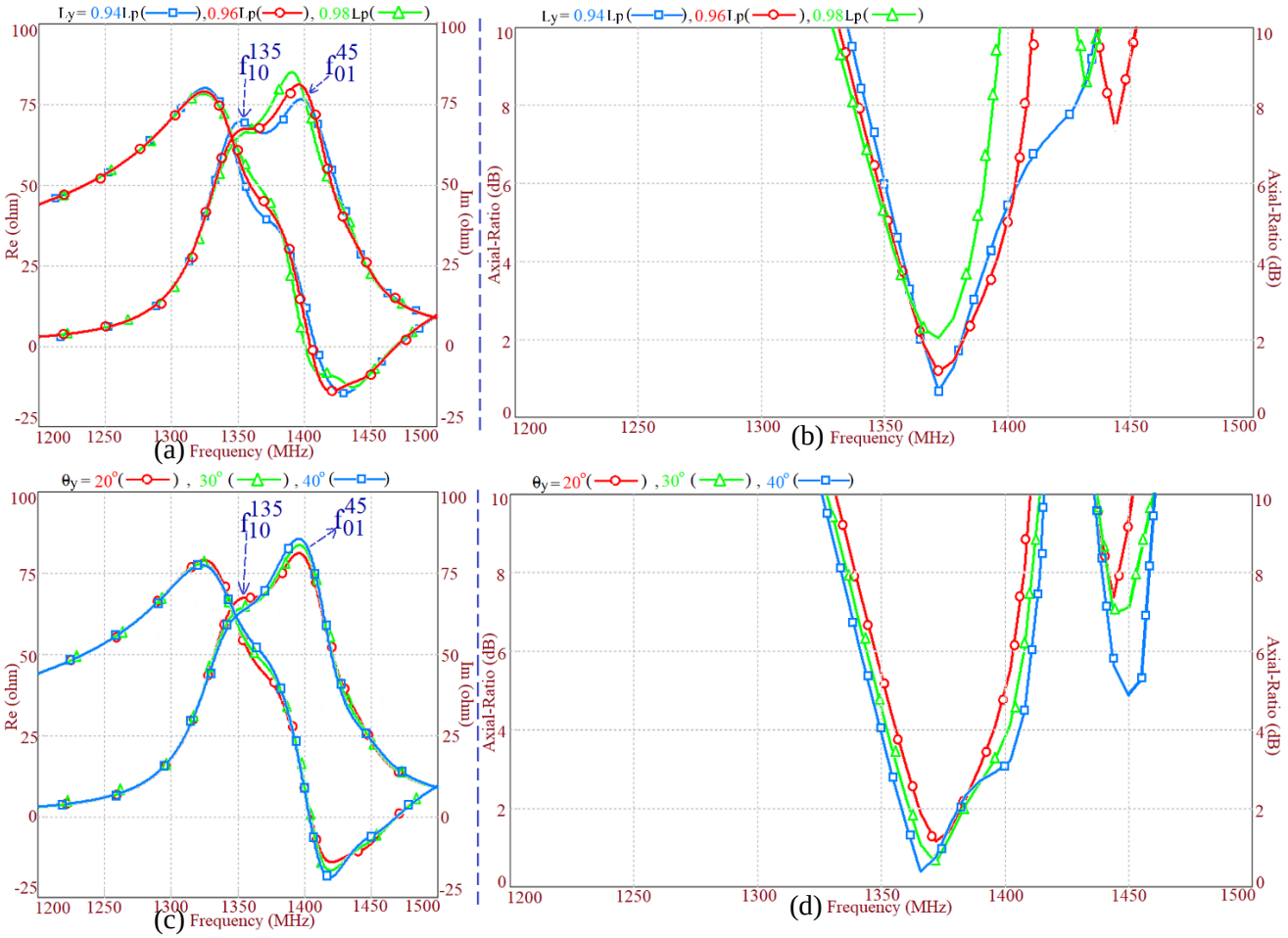

Figure 2. Resonance curve and AR BW plots for the variation in (a), (b) L_y (W_y) and (c), (d) θ_y for the patches gap-coupled along Y-axis.

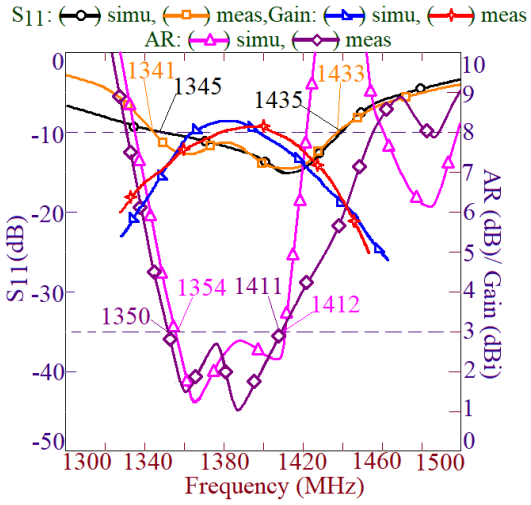

Figure 3. S_{11} & AR BW and gain plots for gap-coupled design of corner truncated SMSA along y-axis.

suspended configuration is selected in which an FR4 substrate of thickness 'h' is suspended above the ground plane using an air gap 'h_a' cm. The total substrate thickness h_t ($h + h_a$) in the original and thus in the redesigned antenna is $0.027\lambda_g$. Here, λ_g is the wavelength in the substrate for the calculated TM_{10} mode frequency as mentioned in Equation (2). For its calculation, the initial value of an effective electric constant (ε_{re}) in the suspended dielectric substrate is unknown as the initial value of h_a is not available. Therefore, the initial assumption of ε_{re} as 1.55 is considered, using which h_t is calculated. From this calculated value of h_t, h_a value that is practically realizable at the said frequency is found out. From this value of h_a, the value of ε_{re} is recalculated using Equation (3). For the total substrate thickness of $0.027\lambda_g$, the recalculated value of ε_{re} marginally varies from the initial approximation. Hence, the new value of ε_{re} is retained in further calculations. The patch length L_p is calculated using Equation (4), and width W_p is selected equal to L_p. The truncation length d is selected as $0.107L_p$, and the feed is placed at $x_f = 0.268L_p$ from the center.

$$f_{10} = f_{\mathrm{AR}}/1.0215 \tag{1}$$

$$\lambda_g = c/f_{10}\sqrt{\varepsilon_{re}} \tag{2}$$

$$\varepsilon_{re} = \frac{\varepsilon_r\,(h + h_a)}{h + h_a\varepsilon_r} \tag{3}$$

$$L_p = (c/2f_{10}\sqrt{\varepsilon_{re}}\,) - (2\,(h + h_a)\,/\sqrt{\varepsilon_{re}}\,) \tag{4}$$

The antenna is designed using these guidelines for $f_{\mathrm{AR}} = 2400$ MHz, and various antenna parameters are $h = 0.16$, $h_a = 0.16$, $W_p = L_p = 4.5$, $d = 0.5$, $x_f = 1.2$ cm. Their results are provided in Fig. 4. The simulated and measured impedance BWs for $S_{11} < -10$ dB are 177 MHz (7.486%) and 182 MHz (7.712%), respectively. The CP AR BWs observed in the simulation and measurement are 42 MHz (1.813%) and 44 MHz (1.905%), respectively. The center frequency of the AR BW in simulation and measurement is near the desired frequency of 2400 MHz. The peak antenna gain is above 7 dBi over the AR BW. The pattern plots show broadside radiation. Since the antenna offers CP radiation, the co- and cross-polarization levels are the same as that observed in the broadside direction. Further, for the given feed point location, the antenna shows left hand CP (LHCP) radiation.

For the same feed patch parameters and by using the relations as $L_y = W_y = 0.93W_p$, $d_y = 0.1W_y$, $\theta_y = 40^\circ$, dimensions of the parasitic patches and their angular rotation with respect to fed patch are calculated. These dimensional relations of the parasitic patches are the same as that presented in the above design of gap-coupled truncated corner square patches along the y-axis. Parasitic patch dimensions in the gap-coupled design along y-axis at 2400 MHz are $W_y = L_y = 4.2$, $d_y = 0.4$ cm. The results are shown in Fig. 5. The simulated and measured impedance BWs are 191 MHz (7.91%) and 207 MHz (8.61%), respectively. The CP AR BWs observed in the simulation and measurement are 113 MHz (4.697%) and 111 MHz (4.633%), respectively. The peak antenna gain is around 7 dBi over the AR BW. The pattern plots show broadside radiation with a higher cross polar component, which is attributed to the CP nature of radiation from the gap-coupled antenna. Across the complete AR BW, the antenna shows LHCP radiation. In the single patch and gap-coupled design (Figs. 6(a), (b)), surface current shows clockwise rotation of the current components indicating the presence of LHCP radiation. With reference to the center frequency of the AR BW, substrate thickness is lower than $0.03\lambda_g$, due to which the AR BW is not more than 5%. To increase the AR BW, a thicker substrate and proximity feeding is selected in the gap-coupled corner truncated SMSAs design as discussed in the following section.

4. PROXIMITY FED GAP-COUPLED DESIGNS OF CORNER TRUNCATED SMSAS

The gap-coupled design of proximity fed corner truncated SMSAs is shown in Figs. 6(c), (d). To increase the AR BW, a thicker substrate is used, and for the input impedance matching, proximity feeding is selected. Initially, a single proximity fed SMSA and its corner truncated variation are studied.

On total substrate thickness of 1.86 cm ($h_a = 1.7$ cm), SMSA dimensions are selected such that its TM_{10} mode frequency is around 2100 MHz. For these antenna parameters, SMSA length is found to be $L_p = 4$ cm. In the above thinner substrate design, it is noted that f_{AR} is larger than the TM_{10} mode frequency of the square patch. Since the targeted frequency band for proximity fed CP SMSAs is

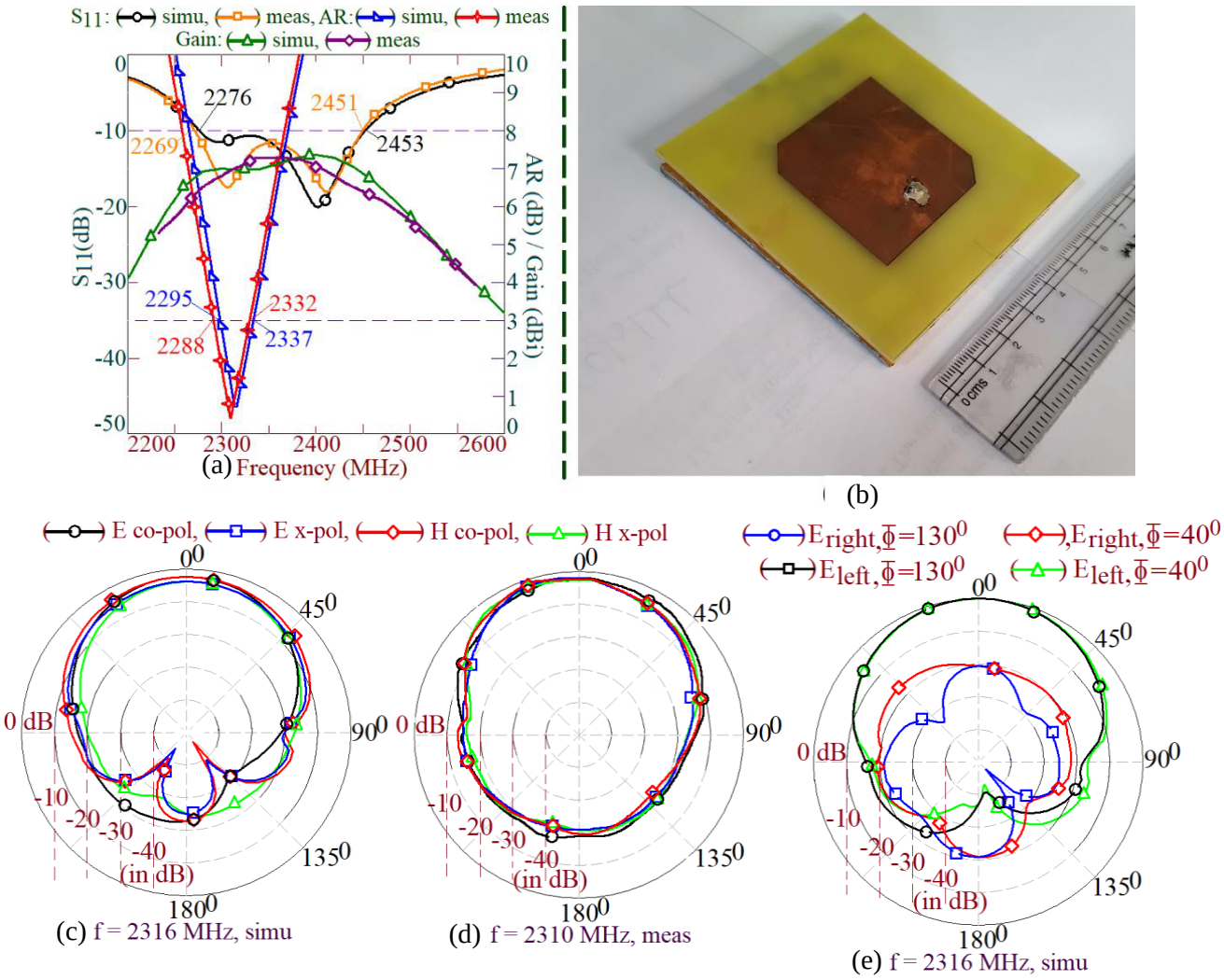

Figure 4. (a) S_{11} and AR BW and gain plots, (b) fabricated prototype, (c), (d) radiation pattern and (e) polarization plot at the center frequency of AR BW for corner truncated SMSA at $f_{\mathrm{AR}} = 2400$ MHz.

2400 MHz, the TM_{10} mode frequency is selected to be lower than the same. By employing the parametric study for the corner truncation 'd', single patch design is optimized for the CP BW.

For $d = 1.15$, $x_f = 1.6$ cm, it yields simulated AR BW of 266 MHz (10.835%), which lies inside the impedance BW of 885 MHz (38.5%). Across the AR BW, single patch design yields the peak broadside gain above 7 dBi. To increase the AR BW, gap-coupled configurations of corner truncated SMSA with parasitic patches are studied. The configurations with patches along x, y and x & y axes are investigated. In each design, to maximize the AR BW, a parametric study for the variation in parasitic patch dimensions (W_x, L_x, W_y, L_y), their spacing with respect to fed SMSA, and an angular rotation with respect to the fed patch (θ_x, θ_y) is carried out. The design with patches gap-coupled along x-axis offers simulated AR BW of 166 MHz (7.18%) that lies inside the impedance BW of 782 MHz (35.37%). Here, peak antenna gain across the AR BW is above 7 dBi. With the patches gap-coupled along x & y axes, a variation in the broadside gain of more than 5 dBi across the AR BW is noted, hence their results are not presented. Optimum results are obtained in the design with patches along the y-axis. Antenna parameters in this design are $W_p = L_p = 4.0$, $W_y = L_y = 3.0$, $x_f = 1.6$, $L_s = 0.6$, $h_s = 1.6$, $d = 1.15$, $d_y = 0.8$ cm, and their results are presented in Figs. 7 & 8. The MSA offers simulated and measured impedance BWs for $S_{11} < -10$ dB of 1213 MHz (49.3%) and 1203 MHz (49.29%), respectively.

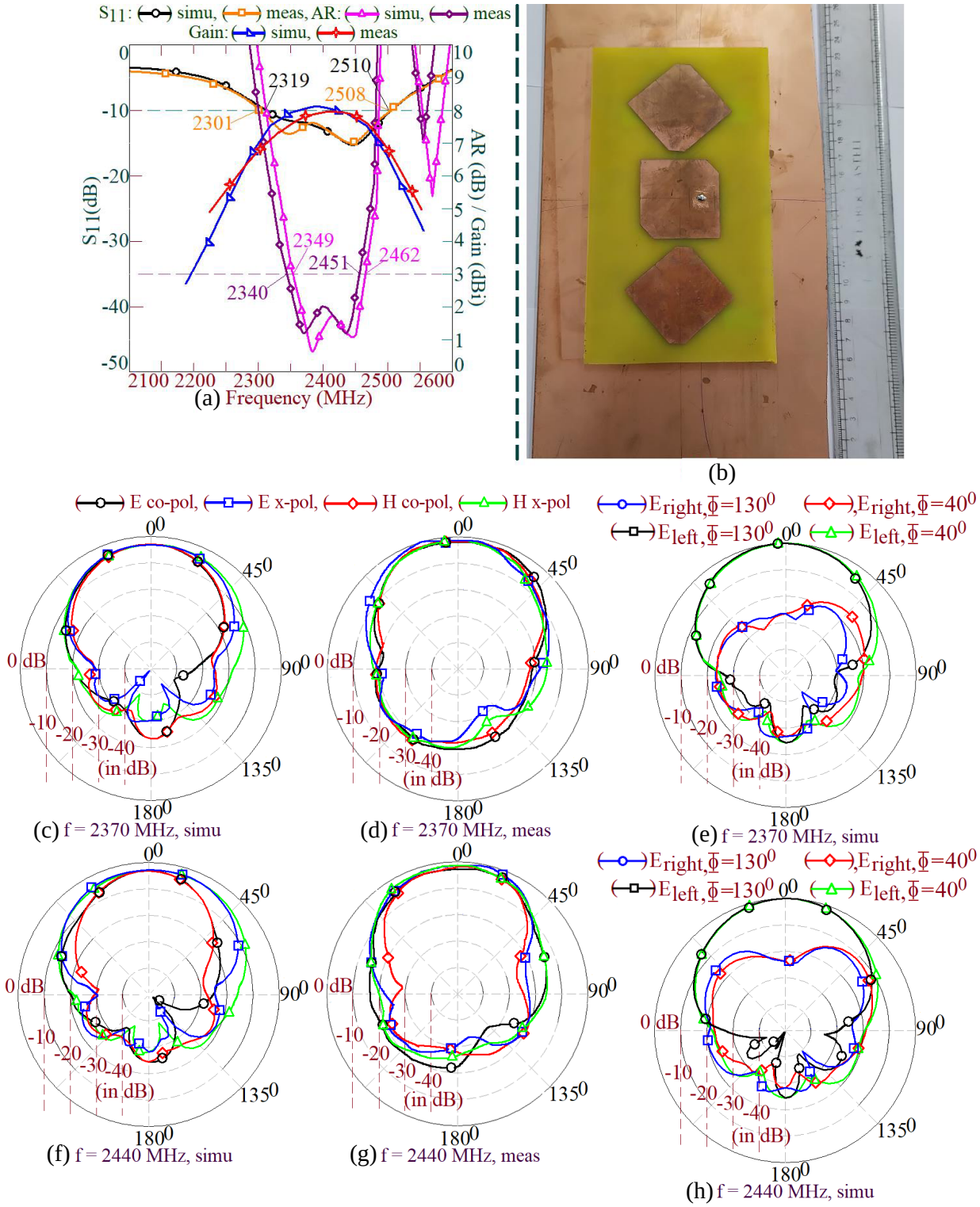

Figure 5. (a) S_{11} and AR BW and gain plots, (b) fabricated prototype, (c)–(h) radiation pattern and polarization plots nearer to the band start and stop frequencies of AR BW for corner truncated SMSA gap-coupled along y-axis for $f_{\mathrm{AR}} = 2400\,\mathrm{MHz}$.

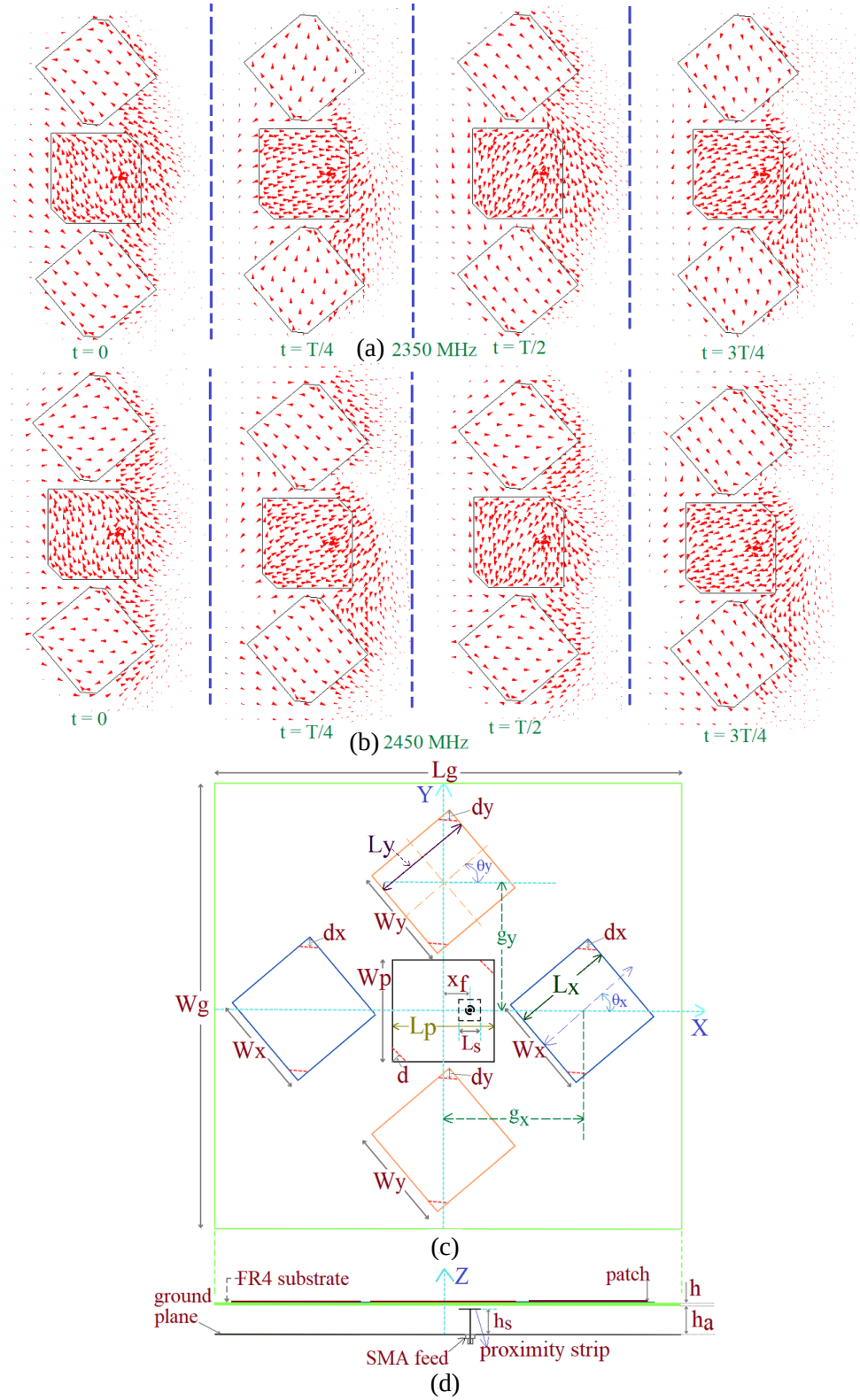

Figure 6. Time varying surface current distribution over the patch nearer to the (a) band start, and (b) band stop frequencies of the AR BW for corner truncated SMSAs gap-coupled along y-axis, for $f_{AR} = 2400$ MHz, (c), (d) proximity fed gap-coupled corner truncated SMSAs.

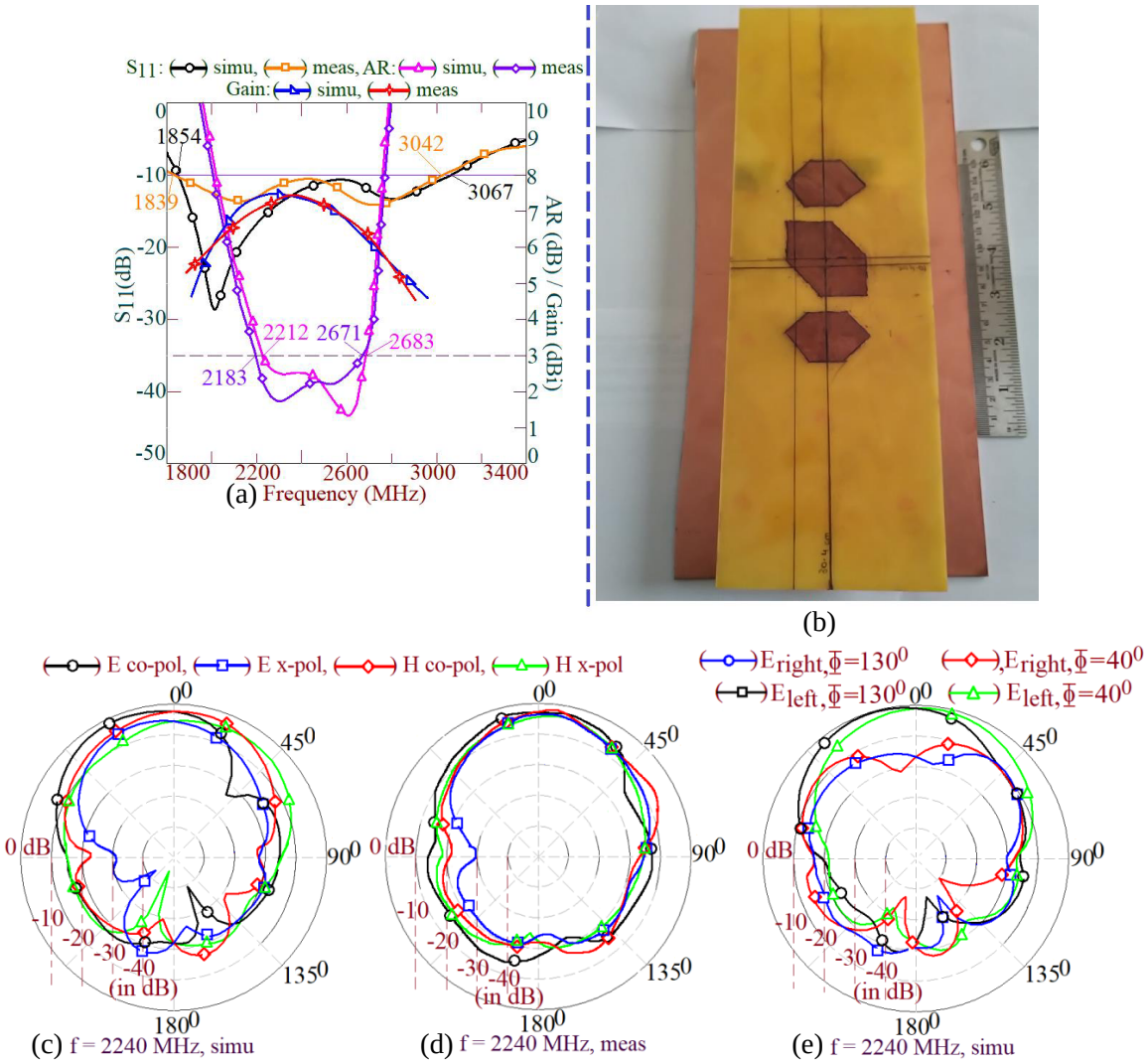

Figure 7. (a) S_{11} BW & gain plots, (b) fabricated antenna, (c), (d) radiation pattern and (e) field polarization plots nearer to the band start frequency of AR BW for proximity fed gap-coupled corner truncated SMSAs along y-axis.

Respective AR BWs for < 3 dB, observed in the simulation and measurement are 471 MHz (19.24%) and 488 MHz (20.11%).

The antenna exhibits broadside gain of greater than 7 dBi across the AR BW. It shows broadside radiation pattern with nearly equal contribution of co- and cross-polarization levels. The presence of equal co- and cross-polarization components indicates the presence of CP radiation. This is further confirmed from the simulated polarization plots and orthogonal E-fields and their phase plots. In the field polarization plots, left hand field components are dominant, indicating the presence of LHCP wave. Across the AR BW, the orthogonal field components are nearly equal in magnitude with a phase difference between them around 90°. Thus a simpler gap-coupled method using the proximity feed and a thicker substrate offers an AR BW of nearly 20% with a broadside gain of above 7 dBi.

Above, the radiation pattern plots are shown at the center frequency of AR BW, and with the circularly polarized radiation, equal contributions from co- and cross-polar components are observed. In gap-coupled designs, when the patches are gap-coupled along a particular axis, a lower beam-width of the pattern in that plane of radiation is observed as compared to its orthogonal plane [1]. However, this is true for the patch having unidirectional surface currents with a single mode excitation, when a linearly

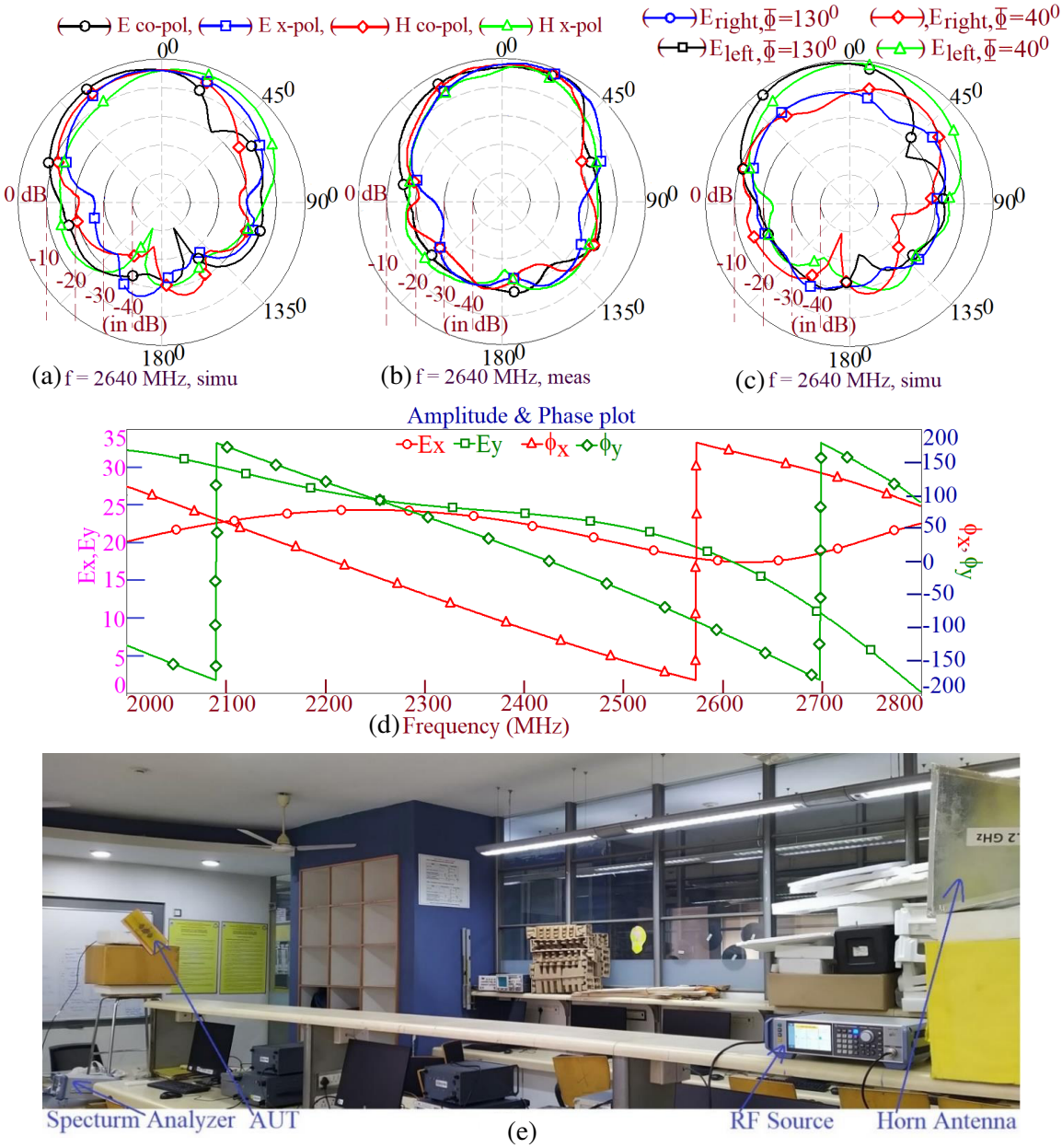

Figure 8. (a), (b) Radiation pattern, (c) field polarization plots nearer to the band start frequency of the AR BW, (d) orthogonal fields and phase plots for proximity fed gap-coupled corner truncated SMSAs along y-axis, and (e) measurement setup for the radiation pattern and broadside gain.

polarized radiation pattern is noted. In the present designs, over the AR BW as orthogonal modes are present, surface currents show bi-directional variations over the fed and parasitic patches. With this lowering of the beam-width in the radiation pattern plot in the plane where gap-coupled patches are present (H-plane) against that in the orthogonal plane (E-plane), beam-width is not significantly noticed. In the above gap-coupled designs maximum possible AR BW is targeted, and thus over the CP BW, AR value is not close to unity. To achieve the AR value close to unity, truncation length on fed and parasitic patches can be altered. However, this will not yield maximum AR BW. Experimental setup for the radiation pattern and gain measurement is shown in Fig. 8(e). A reference wideband Horn antenna is selected. The required minimum far field distance is maintained between the antenna under

test (AUT) and the Horn. This distance is calculated with reference to the highest frequency of the measurement. Around the measurement desk, reflecting metal objects are absent. Also, the distance of the surrounding objects with reference to the measuring desk is more than eight times of the wavelength, being calculated with reference to the lowest frequency of measurement.

5. DESIGN METHODOLOGY FOR PROXIMITY FED GAP-COUPLED CORNER TRUNCATED SMSAS

The design methodology for the proximity fed design is similar to its thinner substrate variation. Minor changes in it are attributed to the thicker substrate being used. The design is initiated by specifying the center frequency of the AR BW, f_{AR}. This frequency can be as per the specific application in consideration. Using this value of f_{AR} and Equation (5), TM_{10} mode frequency of the fed square patch without the corner truncation is obtained. With respect to this TM_{10} mode frequency, a substrate of thickness $0.137\lambda_g$ is selected. Here, λ_g is the wavelength at the calculated TM_{10} mode frequency. Equation (2) is used to evaluate λ_g. As a thicker substrate is selected, $\varepsilon_{re} = 1.055$ is taken as the initial approximation. Using $h_t = 0.137\lambda_g$, the total substrate thickness is obtained. Since $h_t = h_a + h$, for FR4 substrate ($h = 0.16\,\mathrm{cm}$), a practically realizable value of h_a is selected. ε_{re} is recalculated using h_a, by using Equation (3). The recalculated value marginally differs from the initial approximation of ε_{re}. Therefore, the recalculated value of ε_{re} is retained in further calculations. By using Equation (6), patch length L_p is obtained. The patch width is taken equal to its length. The corner truncation length (d) in fed SMSA degenerates the TM_{10} mode into diagonally directed orthogonal modes, TM_{10}^{135} and TM_{01}^{45}. With the corner truncation, the frequency of TM_{01}^{45} is larger than TM_{10}^{135}. In the optimum proximity fed design above, TM_{01}^{45} mode frequency bears a frequency ratio of 1.2245, as mentioned in Equation (7). By using Equations (7)–(9), fed patch truncation length 'd' is evaluated. Further, the proximity feeding strip parameters are selected as $x_f = 0.4L_p$, $h_s = 0.118\lambda_g$, $L_s = 0.15L$. The length (L_y) and width (W_y) of the patches gap-coupled along y-axis are selected as $0.75L_p$. The corner truncation dimension is taken as $d_y = 0.2667L_y$. The patches are placed at distance of $g_y = 2.2h_t$, measured from the fed patch center. The angular rotation in between the fed and parasitic patches is kept to be $\theta_y = 40^\circ$.

$$f_{10} = f_{\mathrm{AR}}/1.139 \tag{5}$$

$$L_p = \left(c/2f_{10}\sqrt{\varepsilon_{re}}\right) - \left(1.5\left(h + h_a\right)/\sqrt{\varepsilon_{re}}\right) \tag{6}$$

$$f_{01}^{45} = 1.2245 f_{10} \tag{7}$$

$$L_d^{45} = \left(c/2f_{01}^{45}\sqrt{\varepsilon_{re}}\right) - \left(1.2\left(h + h_a\right)/\sqrt{\varepsilon_{re}}\right) \tag{8}$$

$$d = L\sqrt{2} - L_d^{45}/2 \tag{9}$$

Using the above methodology, a gap-coupled corner truncated SMSA is designed for $f_{\mathrm{AR}} = 1300\,\mathrm{MHz}$, and various antenna parameters in it are $L_p = W_p = 7.7$, $d = 2.25$, $W_y = L_y = 5.75$, $d_y = 1.55$, $x_f = 3.0$, $L_s = 1.15$, $h_s = 3.05$, $g_y = 7.85\,\mathrm{cm}$. The redesigned antenna offers simulated and measured impedance BWs of 735 MHz (50.39%) and 748 MHz (51%), respectively. The AR BWs observed in the simulation and measurement are 272 MHz (19.88%) and 280 MHz (20%), respectively. The center frequency of AR BW is 1365 MHz, which is close to the desired frequency. The antenna offers similar radiation pattern and gain characteristics to that by above proximity fed design. Thus using the proposed design methodology, a proximity fed antenna can be designed around the given center frequency of the AR BW, which can coincide with the specific wireless application.

6. RESULTS DISCUSSION AND COMPARATIVE ANALYSIS

In this paper, a gap-coupled design using corner truncated SMSAs along the y-axis yields an optimum result. The design using proximity feeding yields an AR BW of nearly 20%. Hence to present the novelty in the proposed work, its results are compared against the reported CP MSAs as discussed in Table 1. The comparison is presented based on the measured impedance and AR BW achieved against the antenna volume and peak gain. The compared configurations have been reported in different frequency ranges. Therefore, to compare the antenna volume, total patch area (A_P) and substrate thickness (h_t) are normalized with reference to the wavelength ($\lambda_{c\mathrm{AR}}$) at the center frequency of the AR BW.

Table 1. Comparison for proximity fed gap-coupled CP MSA against reported CP MSAs.

MSA shown in	Meas. BW (MHz, %)	Meas. AR BW (MHz, %)	Peak Gain (dBi)	Patch Area (A_p/λ_{cAR})	Substrate thickness (h_t/λ_{cAR})
Figs. 6(c), (d)	**1203, 49.29**	**488, 20.11**	**7.5**	**3.83**	**0.14**
Ref. [4]	75, 3.15	40, 1.673	5	4.8	0.02
Ref. [5]	360, 9	350, 8.8	5.8	3.42	0.04
Ref. [6]	198, 7.95	18, 0.72	6.03	2.23	0.04
Ref. [7]	350, 6.8	34, 1.33	10.3	1.91	0.04
Ref. [8]	67, 2.72	16, 0.653	7.6	3.5	0.04
Ref. [10]	3179, 109	1890, 95	6.6	4.123	0.068
Ref. [11]	180, 6	100, 3.3	2.7	3.92	0.03
Ref. [12]	35, 2.2	8, 0.5	3.9	5.64	0.02
Ref. [13]	810, 35	130, 5.3	9.0	2.36	0.1
Ref. [14]	2000, 37.66	550, 11.74	7.0	2.25	0.12
Ref. [15]	5580, 86.9	4940, 74.3	7.3	26.6	0.063
Ref. [16]	30, 1.9	6, 0.4	2.3	1.36	0.05
Ref. [17]	80, 4.1	30, 1.54	8.4	5.255	0.05
Ref. [18]	120, 3.06	122, 3.1	10.0	1.615	0.066
Ref. [19]	1650, 30	1600, 29.1	7.05	1.154	0.106
Ref. [20]	999, 52.6	948, 49.9	9.5	14.56	0.138
Ref. [21]	330, 9.36	250, 7.13	7.75	3.856	0.052
Ref. [22]	110, 4.5	130, 5.3	8.3	18.04	0.0363
Ref. [23]	300, 15.2	160, 8.2	7.0	1.352	0.067
Ref. [24]	4280, 104.4	4440, 118.8	13.2	13.495	0.31
Ref. [25]	3080, 63.3	3040, 63.7	17.77	38.3	0.101
Ref. [26]	1047, 42.5	709, 28	7.9	4.687	0.12

The initial CP design using stub or slot discussed in [3, 4] offers smaller AR BW, being fabricated on a thinner substrate. The MSA discussed in [5, 6] employs additional filtering and power divider circuit, thus increasing the design complexity. The CP design discussed in [7, 8] employs shorting post whereas that presented in [9] uses the combination of shorting post, slot, and modified patch geometry, while shorting the patch, boundary conditions on the same change. Therefore, in [7–9] the shorted patch modes that contribute to the reported CP response are not discussed. Further the AR BW realized in [7–9] is smaller. The AR BW realized in [10] is above 90%, but it employs multiple patches, shorting post, and power divider network. The MSA discussed in [11] offers lower AR BW in spite of employing parasitic patches. The AR BW offered by the slot cut designs in [13, 14] is lower than that achieved in the proposed proximity fed configuration. The ground plane slot cut CP design discussed in [15] requires larger antenna size. MSA employing fractal shape slots on the ground plane offers AR BW lower than 1% [16]. Shorted and slot cut triangular patch design discussed in [17] yields AR BW lower than 2%. The polarization reconfigurable design is presented in [18]. It offers smaller AR BW, while using shorted and slot cut design. Wideband CP MSA discussed in [19] employs stacked patches and power divider network to excite the orthogonal modes, whereas MSA presented in [20] needs larger antenna size. While using four radiating patches, the AR BW obtained in the design discussed in [21] is lower than 10%. The gap-coupled design discussed in [22] offers comparable value of the gain on thinner substrate. However, the design employs shorting post and stubs placed on each of the patch edges with

a larger overall patch size. The CP array designs presented in [24, 25] offer substantially higher values of gain and AR BW. However, the overall patch size is large due to the array nature of the design. With the equivalent values of the gain and substrate thickness, the gap-coupled design presented in [26] needs larger antenna size.

As against the reported techniques of wide-band and multi-band CP MSAs, the proposed work employs a simpler gap-coupled technique to enhance the AR BW. The multi-resonator method used here is not new, but the results obtained in terms of AR BW for the given patch size and thickness against the reported work shows an improvement. For the thinner and thicker substrate proximity fed designs, the design methodology to realize similar antenna in specific frequency band is presented. This allows to design a similar wideband CP configuration as per the specific wireless application.

7. CONCLUSIONS

Multi-resonator gap-coupled designs of corner truncated SMSAs for wideband CP response using electrically thinner and thicker substrates are proposed. An optimum response in terms of the AR BW is achieved with the patches coupled along the y-axis. In 2400 MHz frequency band, the design on a thinner substrate ($h_t \sim 0.03\lambda_g$) yields AR BW of 4.6%, whereas that on a thicker substrate ($h_t \sim 0.14\lambda_g$) yields AR BW of 20%. Both the designs offer broadside radiation pattern characteristics with a gain of greater than 7 dBi. The methodology to realize a similar configuration is presented, which is useful in designing a similar antenna as per specific wireless application. With the obtained antenna characteristics, the proposed configurations can find application in WLAN and Bluetooth in 2400 MHz frequency band.

REFERENCES

1. Kumar, G. and K. P. Ray, *Broadband Microstrip Antennas*, Artech House, London, 2003.
2. Wong, K. L., *Compact and Broadband Microstrip Antennas*, John Wiley and Sons, New York, 2002.
3. Lu, J.-H. and K.-L. Wong, "Single-feed circularly polarized equilateral-triangular microstrip antenna with a tuning stub," *IEEE Transaction on Antennas and Propagation*, Vol. 48, No. 12, 1869–1872, 2000.
4. Bernard Loo, B. K., Nasimuddin, and A. Alphones, "An E-shaped slotted-circular patch antenna for circularly polarized radiation and radiofrequency energy harvesting," *Microwave and Optical Technology Letters*, Vol. 58, No. 5, 868–875, 2016.
5. Wu, Q.-S., X. Zhang, and L. Zhu, "Co-design of a wideband circularly polarized filtering patch antenna with three minima in axial ratio response," *IEEE Transaction on Antennas and Propagation*, Vol. 66, No. 10, 5022 – 5030, 2018.
6. Zhao, Z., F. Liu, J. Ren, Y. Liu, and Y. Yin, "Dual-sense circularly polarized antenna with a dual-coupled line," *IEEE Antennas and Wireless Propagation Letters*, Vol. 19, No. 8, 1415–1419, 2020.
7. Zhang, X. and L. Zhu, "High-gain circularly polarized microstrip patch antenna with loading of shorting pins," *IEEE Transaction on Antennas and Propagation*, Vol. 64, No. 6, 2172–2178, 2016.
8. Xiao, Z., L. Zhu, and N.-W. Liu, "Pin-loaded circularly-polarized patch antennas with wide 3-dB axial ratio bandwidth," *IEEE Transaction on Antennas and Propagation*, Vol. 65, No. 2, 521–528, 2017.
9. Yang, H. and X. Liu, "Wearable dual-band and dual-polarized textile antenna for on and off body communications," *IEEE Antennas and Wireless Propagation Letters*, Vol. 19, No. 12, 2324–2328, 2020.
10. Liang, C.-F., Y.-P. Lyu, D. Chen, W. Zhang, and C.-H. Cheng, "A low-profile and wideband circularly polarized patch antenna based on TM_{11} and TM_{21}," *IEEE Transactions on Antennas and Propagation*, Vol. 69, No. 8, 4439–4446, 2021.

11. Lin, J.-F. and Q.-X. Chu, "Enhancing bandwidth of CP microstrip antenna by using parasitic patches in annular sector shapes to control electric field components," *IEEE Antennas and Wireless Propagation Letters*, Vol. 17, No. 5, 924–927, 2018.
12. Shi, Y. and J. Liu, "A circularly polarized octagon-star-shaped microstrip patch antenna with conical radiation pattern," *IEEE Transactions on Antennas and Propagation*, Vol. 66, No. 4, 2073–2078, 2018.
13. Kovitz, J. M., H. Rajagopalan, and Y. Rahmat-Samii, "Circularly polarised half E-shaped patch antenna: A compact and fabrication-friendly design," *IET Microwave Antennas and Propagation*, Vol. 10, No. 9, 932–938, 2016.
14. Deshmukh Amit, A. and A. A. Odhekar, "Dual band circularly polarized modified ψ-shape microstrip antenna," *Progress In Electromagnetics Research C*, Vol. 115, 161–174, 2021.
15. Tu, L. T., H. H. Tran, and H. C. Park, "Simple-structured dual-slot broadband circularly polarized antenna," *IEEE Antennas and Wireless Propagation Letters*, Vol. 17, No. 3, 476–479, 2018.
16. Wei, K., J. Y. Li, L. Wang, R. Xu, and Z. J. Xing, "A new technique to design circularly polarized microstrip antenna by fractal defected ground structure," *IEEE Transaction on Antennas and Propagation*, Vol. 65, No. 7, 3721–3725, 2017.
17. Chen, J., C. Jin, B. Zhang, and Z. Shen, "Combined triangle quarter-wavelength patches and their application to high-gain CP antenna," *IEEE Antennas and Wireless Propagation Letters*, Vol. 19, No. 1, 104–108, 2019.
18. Chen, Q., J. Li, G. Yang, B. Cao, and Z. Zhang, "A polarization-reconfigurable high-gain microstrip antenna," *IEEE Transaction on Antennas and Propagation*, Vol. 67, No. 5, 3461–3466, 2019.
19. Ta, S. X., V. C. Nguyen, B.-T. Nguyen-Thi, T. B. Hoang, A. N. Nguyen, K. K. Nguyen, and C. Dao-Ngoc, "Wideband dual-circularly polarized antennas using aperture-coupled stacked patches and single-section hybrid coupler," *IEEE Access*, Vol. 10, 21883–21891, 2022.
20. Liang, C.-F., Y.-P. Lyu, D. Chen, and C.-H. Cheng, "Wideband circularly polarized stacked patch antenna based on TM_{11} and TM_{10}," *IEEE Transaction on Antennas and Propagation*, Vol. 70, No. 4, 2459–2467, 2022.
21. Wu, Q.-S., X.-Y. Tang, X. Zhang, L. Zhu, G. Zhang, and C.-B. Guo, "Circularly-polarized patch antennas with enhanced bandwidth based on capacitively coupled orthogonal patch radiators," *IEEE Open Journal of Antennas and Propagation*, Vol. 4, 472–483, 2023.
22. Yang, W.-J., Y.-M. Pan, and X.-Y. Zhang, "A single-layer low-profile circularly polarized filtering patch antenna," *IEEE Antennas and Wireless Propagation Letters*, Vol. 20, No. 4, 602–606, 2021.
23. Cheng, G., B. Huang, Z. Huang, and L. Yang, "A high-gain circularly polarized filtering stacked patch antenna," *IEEE Antennas and Wireless Propagation Letters*, Vol. 22, No. 5, 995–999, 2023.
24. Wei, H., Y. He, Y. Li, S.-W. Wong, and L. Zhu, "A compact ultra wideband circularly polarized antenna array with shared partial patches," *IEEE Antennas and Wireless Propagation Letters*, Vol. 20, No. 12, 2280–2284, 2021.
25. Anamika, V., M. Arrawatia, and G. Kumar, "High gain wideband circularly polarized microstrip antenna array," *IEEE Transaction on Antennas and Propagation*, Vol. 70, No. 11, 11183–11187, 2022.
26. Deshmukh Amit, A., A. V. Doshi, and A. Odhekar, "Gap coupled design star shape microstrip antenna for dual band and wide band circular polarized response," *International Journal of RF & Microwave, Computer Aided Engineering*, Vol. 29, No. 5, 664–674, 2019.
27. IE3D Version 12, Zeland Software.